Surface Science 215 (1989) L297–L306
North-Holland, Amsterdam

SURFACE SCIENCE LETTERS

THE DISCREPANCY BETWEEN HELIUM AND ELECTRON/X-RAY DIFFRACTION FROM THE W(001) SURFACE

P.J. ESTRUP

Brown University, Providence, RI 02912, USA

I.K. ROBINSON and J.C. TULLY

AT&T Bell Laboratories, Murray Hill, NJ 07974, USA

Received 16 November 1988; accepted for publication 10 February 1989

We have carried out model calculations of the diffraction of He from W(001) using the gaussian wave packet method. The calculations support the hypothesis that He diffraction features can exhibit substantial shifts towards specular if (1) they appear at "classically forbidden" angles associated with exponentially decreasing "structure factors" and (2) they are broadened by surface disorder such as that resulting from a two-dimensional order–disorder transition. This may account for the recently discovered discrepancy between the apparent surface periodicity of W(001) as determined by He diffraction and LEED/X-ray.

An interesting controversy has been created by some recent studies of the clean W(001) surface: the two-dimensional periodicity found by helium atom diffraction is not the same as that seen by low-energy electron diffraction (LEED) or by glancing-angle X-ray diffraction.

The experiments were done to determine the structure of the reconstructed W(001) surface above the transition temperature $T_c \approx 230$ K where the long-range order changes from $(\sqrt{2} \times \sqrt{2})$ to (1×1) [1,2]. LEED shows that the half-order diffraction spots, characteristic of the low-temperature phase, gradually decrease in peak intensity and broaden as the temperature is raised; however, the peak positions are unchanged, remaining at $\boldsymbol{q} = (n/2, m/2)\boldsymbol{a}^*$. (Here n and m are odd integers and $a^* = 1.99$ Å^{-1} is the reciprocal lattice parameter.) Some recent LEED measurements of the $(\frac{1}{2}\frac{1}{2})$ spot intensity illustrating this behavior are shown in fig. 1a. The He atom diffraction data by Salanon and Lapujoulade [3] also show line broadening above T_c but in addition, in striking contrast to the LEED results, the $(\frac{1}{2}\frac{1}{2})$ peak is observed to shift, a result which was interpreted as due to formation of an incommensurate surface structure [3]. The effect is large: at $T \approx 320$ K the peak has moved from the original position $q = 1.41$ Å^{-1} to $q \cong 1.2$ Å^{-1}, i.e. a shift of about 15%. At 370 K the shift is nearly twice as large. Ernst, Hulpke and Toennies

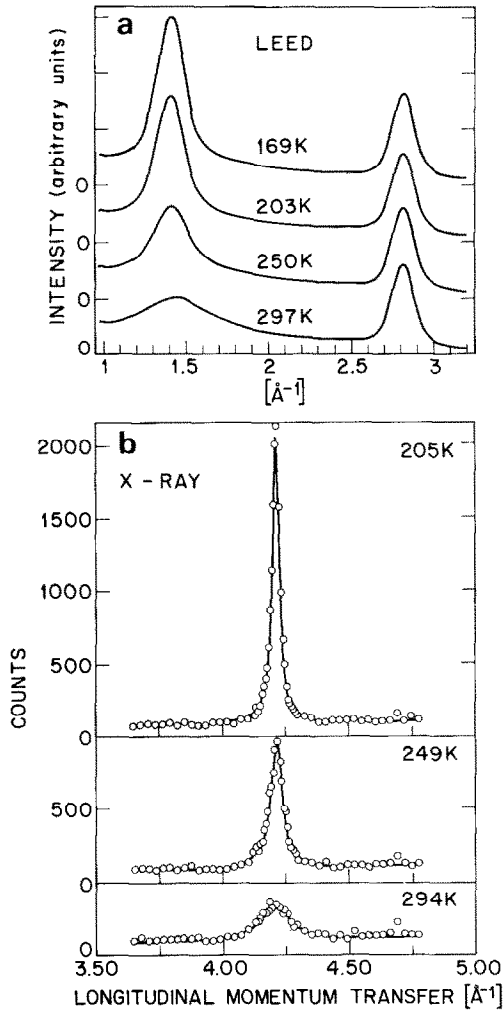

Fig. 1. (a) Low energy electron diffraction from W(001) as a function of surface temperature. (b) Glancing angle X-ray diffraction from W(001) as a function of surface temperature, from ref. [6].

[4], and Schweizer and Rettner [5] very recently have made similar He diffraction experiments on clean W(001) and have confirmed the occurrence of a shift.

To verify that the discrepancy is real we have not only repeated the LEED experiments (fig. 1a) but have also measured the line shape and the positions of the superlattice peaks by means of X-ray diffraction [6,7] to obtain data of high resolution and free of any complications due to multiple scattering. Fig.

1b shows representative X-ray line profiles as a function of temperature. A decrease in the peak intensity accompanied by line broadening is clearly seen, consistent with an order–disorder transition [6,7]. However, within experimental error no shift of the peak occurs [#1].

Thus, the available experimental evidence leads to the conclusion that He atom scattering and electrons/X-ray indeed give different diffraction patterns of W(001) above T_c. The next question is what is the origin of this difference? It has been suggested [8] that the effect is due to inelastic scattering of the He atoms, but the most recent experiments were done with sufficient energy discrimination to rule out this possibility [9]. A more interesting hypothesis [10] is that, whereas the electron and X-ray patterns reflect the W atom core positions, the He pattern is determined by the periodicity of the (conduction) electrons spilling out from the metal into the vacuum. Conceivably these electrons could form a charge density wave incommensurate with the W lattice.

We shall here examine a third possibility, that the He diffraction pattern is distorted because of a strong angle-dependence of the atomic scattering factor. A sufficient reduction of the intensity on the high-angle side of the broadened $(\frac{1}{2}\frac{1}{2})$ peak would result in a shift to lower angle of the observed position of its maximum.

The diffraction of waves from a periodic surface can be described quite generally in the form [11,12]

$$I(\boldsymbol{k}_0, \boldsymbol{k}) \propto |F(\boldsymbol{k}_0, \boldsymbol{k})|^2 |G(\boldsymbol{k}_0, \boldsymbol{k})|^2, \tag{1}$$

where $I(\boldsymbol{k}_0, \boldsymbol{k})$ is the intensity of diffraction in the direction defined by wave vector $\boldsymbol{k} = \boldsymbol{k}_0 + \boldsymbol{q}$ for a wave of incident direction $\boldsymbol{k}_0$. $F(\boldsymbol{k}_0, \boldsymbol{k})$ is the "structure factor" for a single unit cell. $G(\boldsymbol{k}_0, \boldsymbol{k})$ is the interference function which involves a summation over the lattice. For a strictly periodic structure of $M_1 \times M_2$ unit cells,

$$|G(\boldsymbol{k}_0, \boldsymbol{k})|^2 = \frac{\sin^2\left[\frac{1}{2}M_1\boldsymbol{a}_1 \cdot \boldsymbol{q}\right]}{\sin^2\left[\frac{1}{2}\boldsymbol{a}_1 \cdot \boldsymbol{q}\right]} \frac{\sin^2\left[\frac{1}{2}M_2\boldsymbol{a}_2 \cdot \boldsymbol{q}\right]}{\sin^2\left[\frac{1}{2}\boldsymbol{a}_2 \cdot \boldsymbol{q}\right]}, \tag{2}$$

where $\boldsymbol{a}_1$ and $\boldsymbol{a}_2$ are the lattice vectors. For M_1 and M_2 large, eq. (2) approaches a sum of delta functions at the Bragg positions, $\boldsymbol{q} \cdot \boldsymbol{a} = 2n\pi$. Thus for large domain size, the structure factor F controls intensities of diffraction peaks but the positions are fixed by eq. (2). If M_1 and M_2 are not large such as would occur for a disordered surface, then $G(\boldsymbol{k}_0, \boldsymbol{k})$ will still peak at the Bragg positions, but the peaks will have substantial widths. If the structure factor $F(\boldsymbol{k}_0, \boldsymbol{k})$ varies strongly with $\boldsymbol{k}$ in the vicinity of a diffraction peak, then the position of the maximum could shift significantly from the Bragg

[#1] The predicted change in $\boldsymbol{q}$ due to thermal expansion of the crystal is observed; in the temperature interval of interest it is less than 0.05 Å^{-1}.

position. For LEED and X-ray diffraction, the structure factor is generally a relatively slowly varying function of $\boldsymbol{k}$, and it is expected that diffraction peaks will simply broaden for finite domain size, with the maximum remaining essentially at the Bragg positions. For He diffraction [12] the structure factor can depend quite strongly on $\boldsymbol{k}$, resulting in shifts of the diffraction maxima with increasing temperature as domain size is reduced. Whether in practice such shifts can be of the magnitude observed for He diffraction from W(001) [3–5] is a quantitative question. We present below a model calculation of the diffraction from reconstructed W(001) in order to investigate the magnitude of the $\boldsymbol{k}$ dependence of the structure factor for this system.

The calculations employ the gaussian wave packet method exactly as presented by Drolshagen and Heller (DH) [12]. The gaussian wave packet method is advantageous for this application because it affords a direct calculation of the structure factor $F(\boldsymbol{k}_0, \boldsymbol{k})$ which can then be combined with any assumed interference function $G(\boldsymbol{k}_0, \boldsymbol{k})$; i.e., broadening of the diffraction features can be incorporated correctly. We use a rigid gas–surface interaction potential which is a simple extension of that used by DH:

$$V(\boldsymbol{r}) = V_0(z) + V_1(z)Q_1(x, y) + V_2(z)Q_2(x, y), \tag{3}$$

where z is the direction normal to the surface plane, x and y define the [100] and [010] directions in the surface plane, and

$$V_0(z) = D\{\exp[-2\alpha(z - z_0)] - 2\exp[-\alpha(z - z_0)]\}, \tag{4}$$

$$V_1(z) = -2\beta D\exp[-2\alpha(z - z_0)], \tag{5}$$

$$V_2(z) = -2\gamma D\exp[-2\alpha(z - z_0)], \tag{6}$$

$$Q_1(x, y) = \cos(2\pi x/a) + \cos(2\pi y/a), \tag{7}$$

$$Q_2(x, y) = \sin[\pi(x + y)/a]. \tag{8}$$

The first two terms of eq. (3) with eqs. (4), (5), and (7) comprise the DH potential. The last term of eq. (3) with eqs. (6) and (8) break the 1×1 symmetry of the (001) surface, producing the desired $\sqrt{2} \times \sqrt{2}$ reconstruction. The parameters were chosen as follows: The lattice parameter a is 3.164 Å for W(001); the Morse potential parameters, eq. (4), were taken to be the same as employed by DH, $D = 7.63$ meV, $\alpha = 1.1$ Å and $z_0 = 1$ Å. The only remaining parameters are the corrugation parameters β and γ. The ratio γ/β was chosen to be 0.6 in order to approximate the experimentally determined reconstruction of W($\sqrt{2} \times \sqrt{2}$). This ratio produces a shift of the corrugation maxima (i.e., "atom positions") of about 0.2 Å parallel to [110], with alternating signs along [1$\bar{1}$0] to form zig-zag chains in accord with the X-ray determination of Altman et al. [13]. The magnitude of β was chosen to be 0.0075, resulting in $\gamma = 0.0045$, in order to produce a corrugation sufficiently weak that the $(\frac{1}{2}\,\frac{1}{2})$ diffraction peak is classically forbidden, but strong enough so that the

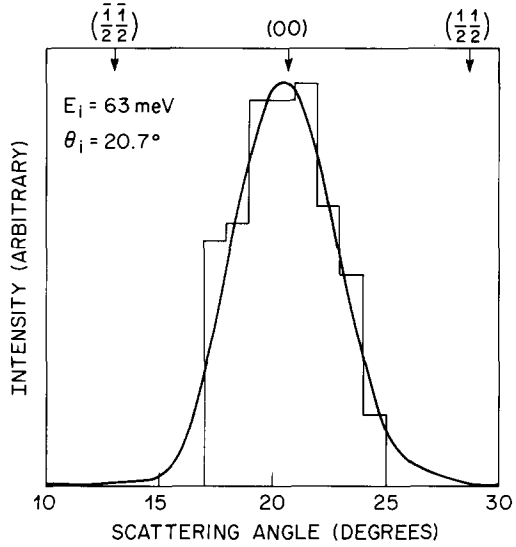

Fig. 2. The solid curve is the calculated structure factor, $|F(\boldsymbol{k}_0, \boldsymbol{k})|^2$, for incident energy $E_i = 63$ meV and incidence angle $\theta_i = 20.7°$ (the conditions of ref. [3]). The arrows show the positions of the maxima in the interference function $|G(\boldsymbol{k}, \boldsymbol{k})|^2$. The histogram is the classical mechanical angular distribution obtained by "binning" the same 256 trajectories employed for the gaussian wave packet calculation.

quantum calculation produces considerable intensity at this position. These parameters result in a corrugation about a factor of two smaller than that postulated by DH for metal surfaces.

The gaussian wave packet approach was implemented exactly as outlined by DH, with the evolution of the wave packets calculated using analytic derivatives. A grid of 16×16 equally spaced wave packets was computed. The initial position–momentum correlation of each packet was chosen so that a packet moving in free space would be optimally focused at the instant of impact with the surface. Setting $\gamma = 0$ and choosing other parameters the same as DH produced quantitative agreement with the results reported by DH.

The smooth curve of fig. 2 is the structure factor $|F(\boldsymbol{k}_0, \boldsymbol{k})|^2$ calculated by the gaussian wave packet method for He scattered from W(001) with initial translational energy $E_i = 63$ meV, incidence angle $\theta_i = 20.7°$ and azimuthal angle $\phi_i = 45°$ (i.e., incident along [110]). These are the conditions of Salanon and Lapujoulade [3]. The histogram is the classical angular distribution obtained from the same 256 trajectories employed for the wave packet calculations. Note that there is no classical intensity at the $(\frac{1}{2}\frac{1}{2})$ angle. The structure factor has significant intensity at the $(\frac{1}{2}\frac{1}{2})$ position, but is decreasing rapidly in this region. The experimentally observed scattering patterns are

presumably a sum of the scattering for two types of domains rotated by 90°, one giving the $(\frac{1}{2}\frac{1}{2})$ and the other the $(\frac{1}{2}\bar{\frac{1}{2}})$ peak. In fig. 2 we show only the dominant $(\frac{1}{2}\frac{1}{2})$ contribution. With our choice of coordinates, the $(\frac{1}{2}\frac{1}{2})$ direction is perpendicular to the zig-zag rows and is thus the "rough" direction responsible for most of the scattering intensity. Scattering in the $(\frac{1}{2}\bar{\frac{1}{2}})$ direction is qualitatively similar, however, and its inclusion would not have changed the results significantly.

In order to calculate the scattering distribution, the structure factor shown in fig. 2 must be multiplied by the interference function as in eq. (1); for a fixed domain size, the latter is given by eq. (2). However, it is more reasonable to assume a distribution of domain sizes, in which case some weighted average

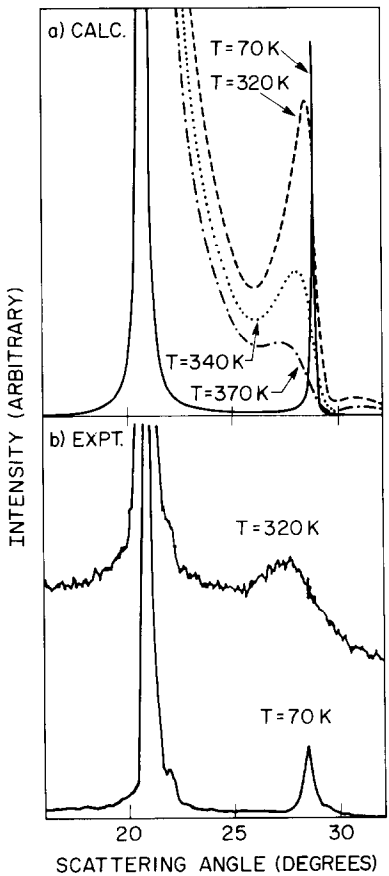

Fig. 3. (a) Calculated scattering distributions for $E_i = 63$ meV and $\theta_i = 20.7°$, obtained by multiplying $|F(\boldsymbol{k}_0, \boldsymbol{k})|^2$ of fig. 2 by the Lorentzian of eq. (9), with temperature dependent half-widths ξ given in table 1. (b) Experimental scattering distributions from ref. [3].

of terms with different M_1 and M_2 must be assumed. Rather than make an arbitrary assumption about the form of $G(\boldsymbol{k}, \boldsymbol{k}_0)$, we simply use the experimental form as determined by X-ray diffraction [6,7]. The X-ray peak shapes are well approximated by Lorentzian form,

$$|G(\boldsymbol{k}_0, \boldsymbol{k})|^2 = A/(1 + \xi^{-2}q^2). \tag{9}$$

The values of the half-widths, ξ, as a function of temperature were taken from the X-ray measurements [6]. In Å^{-1}, they are 0.01, 0.04, 0.09, 0.14 and 0.25 for $T_s = 230$, 280, 320, 340 and 370 K, respectively.

Thus we simply assume a Lorentzian shape for the interference function at the $(\frac{1}{2}\,\frac{1}{2})$ or $(\frac{1}{2}\,\bar{\frac{1}{2}})$ positions, and investigate the shift in the position of the intensity maxima as a function of the width of the Lorentzian, i.e., of temperature. The result for the example of fig. 2 is shown in fig. 3a. At higher temperatures where the linewidth is large due to small domains (small correlation length), the strongly varying structure factor of fig. 2 produces a sizable shift in the position of the intensity maximum of fig. 3a. The shifts are of comparable magnitude to those observed experimentally [3], shown in fig. 3b. Quantitative agreement is neither expected nor found, chiefly due to uncertainties in the assumed interaction potential.

We have also carried out calculations for the conditions of the experiments of refs. [4,5]. The magnitudes of the calculated peak shifts are in rough accord

Table 1
Comparison between experimental and calculated peak shifts

E_i (meV)	θ_i (deg)	T (K)	Peak position (deg)		Half-width (deg)	
			Expt.	Calc.	Expt.	Calc.
63.0	20.7	70	28.8 [a]	28.8	0.3 [a]	0.06
63.0	20.7	280	28.2 [a]	28.7	1.2 [a]	0.24
63.0	20.7	320	27.7 [a]	28.4	1.4 [a]	0.54
63.0	20.7	340	27.3	27.9	1.4 [a]	0.84
63.0	20.7	370	26.5 [a]	27.1	1.4 [a]	1.50
16.8	38.5	220	60.5 [b]	60.5	0.8 [b]	0.2
16.8	38.5	280	58.4 [b]	60.3	3.2 [b]	0.8
16.8	38.5	320	–	59.8	–	1.8
16.8	38.5	340	–	58.9	–	2.9
16.8	38.5	370	55.3 [b]	57.3	6.4 [b]	5.1
27.0	60.0	200	42.7 [c]	42.7	1.8 [c]	0.1
27.0	60.0	270	43.6 [c]	42.8	2.3 [c]	0.3
27.0	60.0	320	44.6 [c]	43.2	2.7 [c]	1.0
27.0	60.0	340	44.9 [c]	43.7	2.8 [c]	1.5
27.0	60.0	370	(45.2) [c]	45.3	(2.9) [c]	2.7

[a] Experimental data from ref. [3].
[b] Experimental data from ref. [4].
[c] Experimental data from ref. [5].

Table 2
Propensity for peak shift, γ, as defined by eq. (10) for $\theta_i = 60°$

E_i (meV)	γ (Å)	E_i (meV)	γ (Å)
27	10	60	12
40	14	90	7

with the experiments for these cases also, using the same interaction parameters. The results are summarized in table 1. The calculated shifts are smaller than the measured shifts at corresponding temperatures in all cases. However, the predicted shifts are sizable and in the right direction. Furthermore, the main reason the calculated shifts are too small is that the X-ray widths employed in the calculations are smaller than the He diffraction widths at the same temperature. If we had employed the He diffraction widths, the calculated shifts would be larger and approximately equal to the experimental shifts. For example, for the incidence conditions $E_i = 16.8$ meV and $\theta_i = 38.5°$, the calculated shift of 1.6° for half-width 2.9° is in good accord with the measured shift of 2.1° for half-width 3.2°. Similar correspondences exist for the other examples of table 1.

It is important to note that the calculated shifts are not too strongly dependent on initial energy or angle; i.e., special conditions are not required for this effect to be large. A measure of the propensity for peak shifts is the slope, γ, of the structure factor at the diffraction position,

$$\gamma = \left(\frac{\mathrm{d} \ln F(\boldsymbol{k}_0, \boldsymbol{k})}{\mathrm{d}\boldsymbol{k}} \right)_{q = 2\pi m/a}. \tag{10}$$

The quantity γ is given in table 2 as a function of incident energy for the $(\frac{1}{2}\frac{1}{2})$ peak at an incidence angle of 60°. A value of γ of 2 Å or higher should yield measurable peak shifts, so from table 2 it is clear that peak shifts should be significant at all incident He atom energies between 20 and 100 meV.

Schweizer and Rettner [5] have measured the diffraction of Ne from W(001). They observe essentially no peak shifts for Ne, in contrast to He scattering at the same incident energy and angle. We have carried out gaussian wave packet calculations for Ne scattering, using the same functional form for the interaction potential, eqs. (3)–(8). The experiments show a much larger effective corrugation for Ne scattering than for He scattering, however. In order to reproduce the overall width of the Ne scattering envelope, we multiplied the He values of the parameters D, β and γ by a factor of 2.4 to obtain the Ne interaction. Ne diffraction patterns as a function of temperature were obtained by multiplying the calculated structure factor by the same Lorentzian functions used for He; the surface domain structure is independent of projectile. The resulting diffraction peaks show negligible shifts with

increasing temperature, in agreement with experiment [5]. The reasons for the large difference in behavior between He and Ne are twofold. Firstly, the increased mass of Ne moves some of the diffraction peaks into the classically allowed center of the structure factor. Secondly, the increased corrugation broadens the classically allowed range of scattering angles. In order for a large peak shift to occur, the structure factor must change by at least a factor of 5 or 10 across the width of the peak; except perhaps for an accidental strong interference minimum, this will generally occur only in the classically forbidden wings of the structure factor.

To conclude, the calculations reported here show that it is plausible that the observed shifts in the He diffraction peaks result simply from line broadening coupled with a steeply decreasing structure factor. There are several caveats, however. First, the accuracy of the gaussian wave packet method has not been established sufficiently, particularly for classically forbidden processes. In the present study the calculated structure factor was found to be relatively insensitive to initial choice of wave packet width for the 63 meV case, but relatively sensitive for the 27 and 16.8 meV cases. Thus we are particularly concerned about the accuracy of the latter. Second, no lattice motion, inelasticity or Debye–Waller effects were included in these calculations. Finally, the gas–surface potential employed here was chosen to make the corrugation strength sufficiently small that scattering at the $(\frac{1}{2}\frac{1}{2})$ angle was classically forbidden, and consequently the quantum intensity very rapidly decreasing in this region. This is consistent with the very small experimental $(\frac{1}{2}\frac{1}{2})$ to (00) intensity ratio. However, the calculations are quite sensitive to the form of the interaction potential and the values of the parameters. We have little confidence in the quantitative aspects of the interaction we have assumed. Thus this calculation in no way establishes the mechanism proposed above as the unique source of or even a significant contributor to the peak shifts observed in He scattering from W(001). Nevertheless, our results demonstrate that realistic gas–surface interactions can give rise to exponential variations of structure factor with angle, particularly in classically forbidden regions. Thus this mechanism cannot be dismissed here, and must be considered in general as a possible source of significant shifts in apparent diffraction peak positions in He scattering from poorly ordered surfaces. Indeed, significant shifts should be the rule rather than the exception for broad, low intensity peaks in the classically forbidden outskirts of the He diffraction envelope.

The LEED data in fig. 1 were obtained by M. Altman. The X-ray data in fig. 2 were obtained in collaboration with M. Altman, R.J. Birgeneau, J.D. Brock, K. Evans-Lutterodt, and A.A. MacDowell. We have benefited from discussions with H.J. Ernst, J.P. Toennies, E.K. Schweizer, R.B. Doak and R.J. Birgeneau. The work at Brown University was supported by National Science Foundation Grant No. DMR 86-15692.

References

[1] T.E. Felter, R.A. Barker and P.J. Estrup, Phys. Rev. Letters 38 (1977) 1138; M.K. Debe and D.A. King, J. Phys. C10 (1977) 1303.
[2] J.E. Inglesfield, Progr. Surface Sci. 20 (1985) 105.
[3] B. Salanon and J. Lapujoulade, Surface Sci. 173 (1986) L613.
[4] H.J. Ernst, E. Hulpke and J.P. Toennies, Phys. Rev. Letters 58 (1987) 1941.
[5] E.K. Schweizer and C.T. Rettner, to be published.
[6] I.K. Robinson, A.A. MacDowell, M.S. Altman, P.J. Estrup, K. Evans-Lutterodt, J.D. Brock and R.J. Birgeneau, to be published.
[7] K. Evans-Lutterodt, R.J. Birgeneau, E.D. Specht, J.W. Chung, J.D. Brock, M.S. Altman, P.J. Estrup, I.K. Robinson and A.A. MacDowell, J. Vacuum Sci. Technol., to be published.
[8] D.A. King, private communication.
[9] H.J. Ernst, private communication.
[10] H.J. Ernst, E. Hulpke and J.P. Toennies, private communication.
[11] G. Ertl and J. Küppers, Low Energy Electrons and Surface Chemistry (VCH, Deerfield Beach, FL, 1985) p. 227 ff.
[12] G. Drolshagen and E.J. Heller, J. Chem. Phys. 79 (1983) 2072.
[13] M.S. Altman, P.J. Estrup and I.K. Robinson, Phys. Rev. B 38 (1988) 5211.